Planar phenomena in *CPT*-even chiral QED with Lorentz violation

J. L. Tomazelli* and G. A. M. A. Fernandes†

Departamento de Física, Universidade Federal de Santa Catarina Caixa Postal 476, CEP 88040-970 Florianópolis, SC, Brazil

(Received 24 March 2019; revised manuscript received 1 May 2019; published 10 June 2019)

Quantum gravity models as string theory, loop quantum gravity, and noncommutative field theories allow for the violation of Lorentz symmetry in the Planck scale. In order to examine the implications of such violation in planar models, we present here a *CPT*-even effective model, in the Standard Model extension framework, for Maxwell-Chern-Simons quantum electrodynamics (QED_3), with a Lorentz violation tensor parameter coupled to the photon field. The magnetoelectric effect induced by the space-time anisotropy in the model is discussed. We then derive the exact classical photon propagator. The electrostatic interaction is investigated and the long-range classical potential, corrected to second order in the Lorentz-violating tensor parameter, is obtained as well as its radiative correction in the isotropic violation scenario, derived at one-loop approximation from the vacuum polarization tensor. Also, the contribution of the space-time anisotropy to the magnetic moment of the fermion trough the vertex diagram is evaluated on shell and in the forward scattering approximation, in the absence of the topological Chern-Simons term.

DOI: 10.1103/PhysRevD.99.115012

I. INTRODUCTION

Lorentz invariance is an important premise of all relativistic theoretical models, having absolute experimental support. However, quantum gravity models as string theory, loop quantum gravity, and noncommutative space-time, predict the violation of this important symmetry in some high energy scale (towards Planck scale), increasing the interest in the physics beyond the Standard Model in the last three decades.

In order to investigate the phenomenological implication of this predicted symmetry loss in the low-energy scale, Colladay and Kostelecky proposed an effective extension to the Standard Model [1–3] where the Lorentz violation occurs via a spontaneous symmetry breaking mechanism, similar to the string field motivated model [4,5], where Lorentz tensors assume vacuum expectation values, establishing preferred directions in space-time and breaking particle Lorentz transformations that are not unitary in the vacuum [1]. These tensors parametrize external fields that couple to the dynamical particle and gauge fields of the Standard Model.

Our interest in the present work is to approach the Lorentz violation in the photon sector of chiral reducible QED_3, highlighting its effect upon the electrostatic interaction of charged particles in the plane and on the magnetic moment of the fermion.

The paper is organized as follows: in Sec. II, we present the model and discuss the magnetoelectric effect induced by the anisotropy in space-time. In Sec. III we determine the exact classical photon propagator, reserving for the Appendix the explicit expressions for its coefficients. Section IV is devoted to the electrostatic potential, were we develop its bare and radiative corrected terms, in one-loop approximation and up to second order in the Lorentz violation parameters, in the presence and in the absence of the Chern-Simons interaction. In Sec. V, the leading contribution to the magnetic moment of the fermion is evaluated on shell and in the forward scattering approximation without taking into account the Chern-Simons term, evidencing the contribution regarding Lorentz violation. We conclude the present investigation with some remarks on the main results and future perspectives.

II. THE MODEL

We studied the extended QED_3 model in the reducible chiral representation given by the following Lagrangian density (with the flat metric $g^{\mu\nu} = \mathrm{diag}(1,-1,-1)$):

$$\begin{aligned} L(x) &= \bar{\psi}(x)(i\partial\!\!\!/ - m_o\tau)\psi(x) - e\bar{\psi}(x)A\!\!\!/(x)\psi(x) \\ &\quad + \frac{1}{2\zeta}(\partial_\mu A^\mu(x))^2 - \frac{1}{4}F^{\mu\nu}(x)F_{\mu\nu}(x) \\ &\quad + \frac{m_{\mathrm{cs}}}{4}\epsilon_{\alpha\beta\lambda}A^\alpha(x)F^{\beta\lambda}(x) - \frac{1}{4}R_{\alpha\beta\mu\nu}F^{\alpha\beta}(x)F^{\mu\nu}(x), \quad (1) \end{aligned}$$

where $\psi(x)$ is the four-component spinor in the reducible representation of QED_3, with the associated 4×4 gamma matrices ($\mu = 0, 1, 2$) defined as in the four-dimensional QED, the matrix $\tau = i\gamma_0\gamma_1\gamma_2$ in the fermion mass term

*jeferson.tomazelli@ufsc.br
†gabrielfsc64@gmail.com

being associated with the Haldane term [6,7,8], the electromagnetic field strength $F^{\mu\nu}(x) = \partial^\mu A^\nu(x) - \partial^\nu A^\mu(x)$ defined by the tripotential $A^\mu(x) = (\phi(x), \vec{A}(x))$; ζ is the gauge-fixing parameter, m_{cs} is the mass parameter related to the Chern-Simons term (which is CPT even in tridimensional space-time), and $R_{\alpha\beta\mu\nu}$ is the constant tensor field that couples to the photon field and parametrizes the Lorentz symmetry breaking, introducing a preferred direction in space-time.

The algebraic relations underlying (1) are summarized by

$$\{\gamma^\mu, \gamma^\nu\} = 2g^{\mu\nu}, \tag{2}$$

$$[\tau, \gamma^\mu] = 0. \tag{3}$$

As its four-dimensional counterpart [2], the Lorentz-violating term introduced in our planar model (1) preserves CPT,

$$\begin{aligned}
&A^1(x^0, x^1, x^2) \xrightarrow{P} -A^1(x^0, -x^1, x^2),\\
&A^{0,2}(x^0, x^1, x^2) \xrightarrow{P} A^{0,2}(x^0, -x^1, x^2)\\
&A^0(x^0, x^1, x^2) \xrightarrow{T} A^0(-x^0, x^1, x^2),\\
&A^{1,2}(x^0, x^1, x^2) \xrightarrow{T} -A^{1,2}(-x^0, x^1, x^2)\\
&A^\mu(x) \xrightarrow{C} -A^\mu(x),
\end{aligned} \tag{4}$$

and the tensor parameter $R_{\alpha\beta\mu\nu}$ exhibits the same properties as the Riemann-Christoffel tensor [9]

$$\begin{aligned}
&R_{\alpha\beta\mu\nu} = -R_{\alpha\beta\nu\mu} = -R_{\beta\alpha\mu\nu}\\
&R_{\alpha\beta\mu\nu} = R_{\mu\nu\alpha\beta}\\
&R_{\alpha\beta\mu\nu} + R_{\alpha\nu\beta\mu} + R_{\alpha\mu\nu\beta} = 0\\
&\partial_\eta R_{\alpha\beta\mu\nu} + \partial_\nu R_{\alpha\beta\eta\mu} + \partial_\mu R_{\alpha\beta\nu\eta} = 0.
\end{aligned} \tag{5}$$

In view of (5), we chose a basis for the tensor $R_{\alpha\beta\mu\nu}$ formed by two linearly independent trivectors[1] u_μ and v_μ as [9]

$$\begin{aligned}
R_{\alpha\lambda\mu\eta} = &\frac{1}{2}(u_\alpha v_\mu + u_\mu v_\alpha)g_{\lambda\eta} + \frac{1}{2}(u_\lambda v_\eta + u_\eta v_\lambda)g_{\alpha\mu}\\
&-\frac{1}{2}(u_\alpha v_\eta + u_\eta v_\alpha)g_{\lambda\mu} - \frac{1}{2}(u_\lambda v_\mu + u_\mu v_\lambda)g_{\alpha\eta}\\
&-\frac{5}{8}u.v(g_{\alpha\mu}g_{\lambda\eta} - g_{\alpha\eta}g_{\lambda\mu}).
\end{aligned} \tag{6}$$

[1] The tensor structure (6) involving u_μ and v_μ components is not the most general, in that it contains five independent parameters in contrast to the six allowed by $R_{\alpha\beta\mu\eta}$ in three dimensions. Physically, this means that we consider 1 "frozen degree of freedom" in the Lorentz-violating parameter space, imposing a constraint among those components, which reflects on the gauge propagator structure, baring a similarity with a particular choice of a noncovariant gauge-fixing term in dealing with the gauge sector of the Standard Model of particle physics.

The proposed planar model (1) comprises a rich phenomenology already in the pure gauge case, as will be briefly discussed next.

A. Magnetoelectric effect

Taking the pure Maxwell part of (1), neglecting the Chern-Simons term for simplicity, leads to the Lagrangian density

$$L_{\rm EM}(x) = -\frac{1}{4}F^{\mu\nu}(x)F_{\mu\nu}(x) - \frac{1}{4}R_{\alpha\beta\mu\nu}F^{\alpha\beta}(x)F^{\mu\nu}(x), \tag{7}$$

which can be written in terms of the electric and magnetic field strengths, $\vec{E}(\vec{r}, t)$ and $B(\vec{r}, t)$, and anisotropy trivectors, u^μ and v^μ, through (6)

$$\begin{aligned}
L_{\rm EM}(\vec{r}, t) = &\frac{1}{2}\left(\frac{5}{4}u.v - 1\right)(B^2(\vec{r}, t) - \vec{E}^2(\vec{r}, t))\\
&+ u^0 v^0 \vec{E}^2(\vec{r}, t) - u^0 B(\vec{r}, t)\vec{v} \times \vec{E}(\vec{r}, t)\\
&- v^0 B(\vec{r}, t)\vec{u} \times \vec{E}(\vec{r}, t)\\
&- \vec{v}.\vec{E}(\vec{r}, t)\vec{u}.\vec{E}(\vec{r}, t) + B^2(\vec{r}, t)\vec{u}.\vec{v},
\end{aligned} \tag{8}$$

where we defined the "vector product" in the tridimensional space-time as $\vec{a} \times \vec{b} = \epsilon^{0ij}a_i b_j$, with the spatial indices $i; j = 1, 2$, resulting in a pseudoscalar.

From (8) follows the electric displacement bivector $\vec{D}(\vec{r}, t) = \partial L_{\rm EM}/\partial\vec{E}$ and the magnetic induction $H(\vec{r}, t) = -\partial L_{\rm EM}/\partial B$, which provide the electric polarization $\vec{P}(\vec{r}, t)$ and magnetization $M(\vec{r}, t)$ of the anisotropic medium through

$$\vec{D} = \vec{E} + 4\pi\vec{P} \tag{9}$$

and

$$H = B - 4\pi M, \tag{10}$$

ending up with

$$\begin{aligned}
P_x = \frac{1}{4\pi}\Big[&-\frac{5}{4}u.vE_x + 2u^0v^0E_x - v_x\vec{u}.\vec{E}\\
&- u_x\vec{v}.\vec{E} + u^0v_yB + v^0u_yB\Big],
\end{aligned} \tag{11}$$

$$\begin{aligned}
P_y = \frac{1}{4\pi}\Big[&-\frac{5}{4}u.vE_y + 2u^0v^0E_y - v_y\vec{u}.\vec{E}\\
&- u_y\vec{v}.\vec{E} - u^0v_xB - v^0u_xB\Big],
\end{aligned} \tag{12}$$

$$M = -\frac{1}{4\pi}\left[-\frac{5}{4}u.vB - 2B\vec{u}.\vec{v} + u^0\vec{v} \times \vec{E} + v^0\vec{u} \times \vec{E}\right]. \tag{13}$$

These expressions reveal that the anisotropy induced by the Lorentz symmetry breaking makes the vacuum behave as a polarizable medium and exhibit the magnetoelectric effect [10,11]; i.e., an electric (magnetic) field generates a magnetization (electric polarization) of the medium, as shown in (11)–(13). Therefore, in the condensed matter scenario, the Lagrangian density (8) can provide an effective model for describing anisotropic planar systems with magnetoelectric capabilities, of interest in magnetic sensor devices.

Another feature of the pure gauge Lorentz-violating model (8) that follows directly from the associated equations of motion is the transversality loss of plane waves, producing transverse magnetic modes in the spatially anisotropic vacuum [8]. In an isotropic vacuum, i.e., $u^\mu = (u^0, \vec{0})$ and $v^\mu = (v^0, \vec{0})$, the transversality of the wave is preserved and the electromagnetic field propagates in the usual transverse electric-magnetic mode [8].

III. PHOTON PROPAGATOR

The photon propagator $D^{\mu\nu}(p)$ of the full model (1) is derived, in momentum space, from the Green's equation associated with the vector field $A^\mu(p)$,

$$[-g_{\alpha\eta}p^2 + \tilde{\zeta} p_\alpha p_\eta - i m_{cs}\epsilon_{\alpha\mu\eta}p^\mu + 2R_{\alpha\lambda\mu\eta}p^\lambda p^\mu]D^{\eta\sigma}(p) = \delta^\sigma_\alpha, \tag{14}$$

where we introduced $\tilde{\zeta} \equiv 1 + 1/\zeta$.

Exploring the tensor structure of our planar model, we proposed the following ansatz for the propagator:

$$\begin{aligned} D^{\eta\sigma}(p) = {} & C_1 g^{\eta\sigma} + C_2 p^\eta p^\sigma + iC_3\epsilon^{\eta\sigma\lambda}p_\lambda + C_4 u^\eta v^\sigma + C_5 u^\sigma v^\eta + C_6 u^\eta u^\sigma + C_7 v^\eta v^\sigma + iC_8\epsilon^{\eta\sigma\lambda}u_\lambda + iC_9\epsilon^{\eta\sigma\lambda}v_\lambda \\ & + iC_{10}(p\times u)^\eta u^\sigma + iC_{11}(p\times u)^\sigma u^\eta + iC_{12}(v\times u)^\eta u^\sigma + iC_{13}(v\times u)^\sigma u^\eta + iC_{14}(v\times p)^\sigma u^\eta + iC_{15}(v\times p)^\eta u^\sigma \\ & + iC_{16}(p\times u)^\eta v^\sigma + iC_{17}(p\times u)^\sigma v^\eta + iC_{18}(v\times u)^\eta v^\sigma + iC_{19}(v\times u)^\sigma v^\eta + iC_{20}(v\times p)^\sigma v^\eta + iC_{21}(v\times p)^\eta v^\sigma \\ & + C_{22}p^\eta u^\sigma + C_{23}u^\eta p^\sigma + C_{24}p^\eta v^\sigma + C_{25}v^\eta p^\sigma + iC_{26}(p\times u)^\eta p^\sigma + iC_{27}(p\times u)^\sigma p^\eta + iC_{28}(p\times v)^\eta p^\sigma \\ & + iC_{29}(p\times v)^\sigma p^\eta + iC_{30}(u\times v)^\sigma p^\eta + iC_{31}(u\times v)^\eta p^\sigma + iC_{32}(u\times v)^\eta (u\times v)^\sigma + iC_{33}(u\times p)^\eta (u\times p)^\sigma \\ & + iC_{34}(v\times p)^\eta (v\times p)^\sigma + iC_{35}(v\times p)^\eta (u\times p)^\sigma + iC_{36}(u\times p)^\eta (v\times p)^\sigma + iC_{37}(v\times p)^\eta (u\times v)^\sigma \\ & + iC_{38}(u\times v)^\eta (v\times p)^\sigma + iC_{39}(u\times v)^\eta (u\times p)^\sigma + iC_{40}(u\times p)^\eta (u\times v)^\sigma, \end{aligned} \tag{15}$$

where the coefficients $C_k \equiv C_k(p)$, with $(k = 1, \ldots, 40)$, are functions of the photon trimomentum p^μ.

With (15), we solved the linear system provided by (14) and obtained originally the exact photon propagator for the Maxwell-Chern-Simons extended QED_3. For brevity, we listed the respective coefficients in the Appendix.

In view of the phenomenological smallness expected for the Lorentz violation quantities u^μ and v^μ, with bounds in four dimensions given in [12], we proceeded with a perturbative expansion for the exact propagator (15) in the anisotropy trivectors, in order to obtain the leading contribution of the Lorentz violation for the planar electrostatic potential. Consequently, up to second order in the trivectors, the photon propagator reduces to

$$\begin{aligned} D^{\eta\sigma}(p) = {} & \left[\frac{1}{m_{\mathrm{cs}}^2 - p^2} + \frac{2}{p^2}\frac{m_{\mathrm{cs}}^2 + p^2}{(m_{\mathrm{cs}}^2 - p^2)^2} p.v p.u - \frac{5}{4}\frac{m_{\mathrm{cs}}^2 + p^2}{(m_{\mathrm{cs}}^2 - p^2)^2} u.v\right] g^{\eta\sigma} + \left[\frac{1}{\tilde{\zeta} - 1}\frac{1}{(p^2)^2} + \frac{1}{p^2}\frac{1}{p^2 - m_{\mathrm{cs}}^2} + \frac{5}{4}\frac{u.v}{(p^2 - m_{\mathrm{cs}}^2)^2}\right] p^\eta p^\sigma \\ & + i\left[\frac{1}{p^2}\frac{m_{\mathrm{cs}}}{m_{\mathrm{cs}}^2 - p^2} - \frac{5}{2}\frac{m_{\mathrm{cs}}}{(m_{\mathrm{cs}}^2 - p^2)^2} u.v + 4\frac{1}{p^2}\frac{m_{\mathrm{cs}}}{(m_{\mathrm{cs}}^2 - p^2)^2} p.u p.v\right]\epsilon^{\eta\sigma\lambda}p_\lambda + \frac{p^2}{(p^2 - m_{\mathrm{cs}}^2)^2}(u^\eta v^\sigma + u^\sigma v^\eta) \\ & - \frac{p.v}{(p^2 - m_{\mathrm{cs}}^2)^2}(p^\eta u^\sigma + p^\sigma u^\eta) - \frac{p.u}{(p^2 - m_{\mathrm{cs}}^2)^2}(p^\eta v^\sigma + p^\sigma v^\eta) - i\frac{m_{\mathrm{cs}}}{(m_{\mathrm{cs}}^2 - p^2)^2}[(v\times p)^\sigma u^\eta - (v\times p)^\eta u^\sigma] \\ & - i\frac{m_{\mathrm{cs}}}{(m_{\mathrm{cs}}^2 - p^2)^2}[(u\times p)^\sigma v^\eta - (u\times p)^\eta v^\sigma] + i\frac{m_{\mathrm{cs}}}{(m_{\mathrm{cs}}^2 - p^2)^2}\frac{p.v}{p^2}[(p\times u)^\eta p^\sigma - (p\times u)^\sigma p^\eta] \\ & + i\frac{m_{\mathrm{cs}}}{(m_{\mathrm{cs}}^2 - p^2)^2}\frac{p.u}{p^2}[(p\times v)^\eta p^\sigma - (p\times v)^\sigma p^\eta] + \frac{m_{\mathrm{cs}}^2}{p^2}\frac{1}{(p^2 - m_{\mathrm{cs}}^2)^2}[(v\times p)^\eta (u\times p)^\sigma + (u\times p)^\eta (v\times p)^\sigma] \\ & + O(u^3, v^3). \end{aligned} \tag{16}$$

IV. ELECTROSTATIC POTENTIAL

From the photon propagator we can obtain information about the electrostatic interaction of charged particles. In this section we will derive the potential produced by a static fermion in the plane, discussing the role of the Chern-Simons term, and the radiative corrections induced by the vacuum fluctuations, identifying the contributions of the anisotropy introduced by the Lorentz violation.

A. Classical Potential

In momentum space, the electrostatic potential produced by a single charged fermion is given by [13]

$$A^0_{\rm cl}(\vec{k}) = -eD_F^{00}(0,\vec{k}). \tag{17}$$

1. Case $m_{\rm cs} \neq 0$

From the photon propagator (16) in the Landau gauge $\tilde{\zeta} = \infty$, the electrostatic potential (17) reads

$$\begin{aligned} A^0_{\rm cl}(\vec{k}) = -e\Bigg\{ &\frac{1}{m_{\rm cs}^2+\vec{k}^2} - \frac{2}{\vec{k}^2}\frac{m_{\rm cs}^2-\vec{k}^2}{(m_{\rm cs}^2+\vec{k}^2)^2}\vec{k}.\vec{v}\,\vec{k}.\vec{u} \\ &-\frac{5}{4}\frac{m_{\rm cs}^2-\vec{k}^2}{(m_{\rm cs}^2+\vec{k}^2)^2}u.v - \frac{2\vec{k}^2}{(\vec{k}^2+m_{\rm cs}^2)^2}u^0v^0 \\ &-\frac{2m_{\rm cs}^2}{\vec{k}^2(\vec{k}^2+m_{\rm cs}^2)^2}|\vec{v}\times\vec{k}||\vec{u}\times\vec{k}|\Bigg\}. \end{aligned} \tag{18}$$

Denoting the fixed angle between the bivectors $\vec{u}$ and $\vec{v}$ by β, the angle between the position vector $\vec{r}$ and the vector $\vec{u}$ by α and the angle between the momentum vector $\vec{k}$ and the vector $\vec{u}$ by θ, as depicted in Fig. 1, we performed the Fourier transform of (18) to the position space,

$$A^0_{\rm cl}(\vec{r}) = \int \frac{d^2\vec{k}}{(2\pi)^2} e^{i\vec{k}.\vec{r}} A^0_{\rm cl}(\vec{k}), \tag{19}$$

obtaining, with use of the software Mathematica,

$$\begin{aligned} A^0_{\rm cl}(\vec{r}) &= -\frac{e}{2\pi}\int_0^\infty \frac{\rho}{1+\rho^2}\mathrm{J}_0(m_{\rm cs}\rho r)d\rho + \frac{e}{2\pi}\frac{u^0v^0}{4}\int_0^\infty\frac{\rho}{(1+\rho^2)^2}(5+3\rho^2)\mathrm{J}_0(m_{\rm cs}\rho r)d\rho \\ &\quad -\frac{e}{4(2\pi)^2}|\vec{v}||\vec{u}|\int_0^\infty\int_0^{2\pi}\rho d\rho d\phi e^{i\rho r\cos(\phi)}\frac{1}{(m_{\rm cs}^2+\rho^2)^2} \\ &\quad \times[(5m_{\rm cs}^2-\rho^2)\cos(\beta) + (-8m_{\rm cs}^2+4\rho^2)\cos(2(\alpha-\phi)-\beta)], \\ &= -\frac{e}{2\pi}\mathrm{K}_0(m_{\rm cs}r) + \frac{e}{8\pi}u^0v^0[3\mathrm{K}_0(m_{\rm cs}r) + m_{\rm cs}r\mathrm{K}_1(m_{\rm cs}r)] \\ &\quad -\frac{e}{8\pi}\cos(\beta)|\vec{v}||\vec{u}|[3m_{\rm cs}r\mathrm{K}_1(m_{\rm cs}r) - \mathrm{K}_0(m_{\rm cs}r)] \\ &\quad -\frac{e}{2\pi}\cos(2\alpha-\beta)|\vec{v}||\vec{u}|\left[-\frac{3}{2}m_{\rm cs}r\mathrm{K}_1(m_{\rm cs}r) - 2\mathrm{K}_2(m_{\rm cs}r) + \frac{4}{m_{\rm cs}^2r^2}\right], \end{aligned} \tag{20}$$

where $J_l(x)$ is the Bessel function of the first kind and order l and $K_l(x)$ is the modified Bessel function of the second kind and order l.

The first term in (20) is the well-known Bessel modified potential of planar Maxwell-Chern-Simons electrodynamics. The second one gives the signature of an isotropic Lorentz symmetry breaking in the electrostatic interaction being sketched in[2] Fig. 2. The remaining terms in (20), sketched in Figs. 3 and 4, carry the influence of spatial anisotropy on the classical potential, manifested as a circularly symmetric contribution and an angular dependency, in the third and fourth terms, respectively.

[2]In all graphs in this section, we are only interested in showing the behavior of the long-range electrostatic potential. Therefore, we sketched all related figures in terms of adimensional quantities, avoiding to attribute values for the physical parameters.

2. Case $m_{\rm cs} = 0$

In the absence of the topological mass, the photon propagator (16) in the Landau gauge becomes

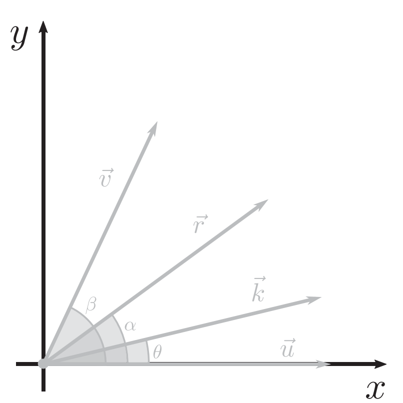

FIG. 1. Angular parametrization of the relevant planar vectors.

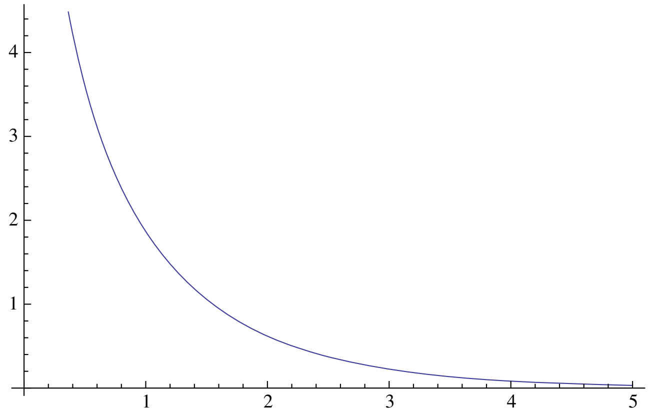

FIG. 2. Contribution to the electrostatic potential $\frac{A^0_{\rm cl}}{(e/8\pi)u^0v^0}$ vs $m_{\rm cs}r$, in the isotropic case with $m_{\rm cs}\neq 0$.

$$
\begin{aligned}
&D^{\eta\sigma}(p;m_{\rm cs}=0)\\
&\quad=-\frac{1}{p^2}\left(g^{\eta\sigma}-\frac{p^\eta p^\sigma}{p^2}\right)-\frac{1}{p^2}\left(g^{\eta\sigma}-\frac{p^\eta p^\sigma}{p^2}\right)\frac{5}{4}u.v\\
&\qquad+2\frac{p.up.v}{(p^2)^2}g^{\eta\sigma}+\frac{1}{p^2}(u^\eta v^\sigma+u^\sigma v^\eta)\\
&\qquad-\frac{1}{(p^2)^2}[p.v(p^\eta u^\sigma+p^\sigma u^\eta)+p.u(p^\eta v^\sigma+p^\sigma v^\eta)]\\
&\qquad+O(u^3,v^3). \qquad (21)
\end{aligned}
$$

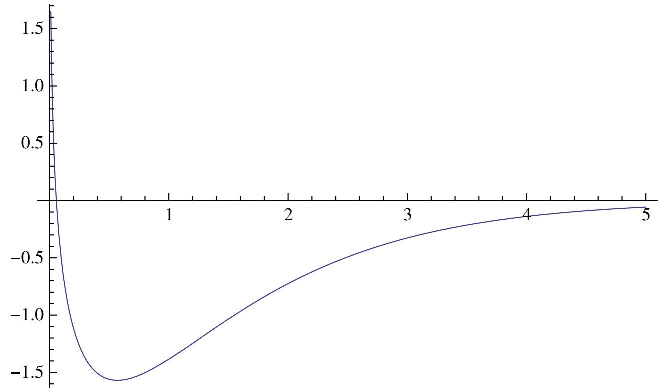

FIG. 3. Circularly symmetric contribution to the electrostatic potential $\frac{A^0_{\rm cl}}{(e/8\pi)|\vec{u}||\vec{v}|}$ vs $m_{\rm cs}r$, in the anisotropic collinear case with $m_{\rm cs}\neq 0$.

Therefore, the momentum-space potential (17) is

$$
A^0_{\rm cl}(\vec{k})=-e\left[\frac{1}{\vec{k}^2}-2\frac{u^0v^0}{\vec{k}^2}+\frac{5}{4}\frac{u.v}{\vec{k}^2}+\frac{2}{(\vec{k}^2)^2}\vec{k}.\vec{u}\,\vec{k}.\vec{v}\right] \qquad (22)
$$

and, performing the Fourier transform, follows the position-space classical electrostatic potential

$$
\begin{aligned}
A^0_{\rm cl}(\vec{r})&=-\frac{e}{2\pi}\left(1-\frac{3}{4}u^0v^0\right)\int_0^\infty\frac{\rho}{\rho^2+m_{ir}^2}\mathrm{J}_0(\rho r)d\rho+\frac{e}{8\pi}|\vec{u}||\vec{v}|\cos(\beta)\int_0^\infty\frac{\rho}{\rho^2+m_{ir}^2}\mathrm{J}_0(\rho r)d\rho\\
&\quad-\frac{e}{(2\pi)^2}|\vec{u}||\vec{v}|\int_0^\infty\int_0^{2\pi}\rho d\rho d\phi e^{i\rho r\cos(\phi)}\frac{1}{\rho^2+m_{ir}^2}\cos[\beta-2(\alpha-\phi)]\\
&=-\frac{e}{2\pi}\left(1-\frac{3}{4}u^0v^0\right)[-\gamma_{\rm euler}+\ln(2)-\ln(r)-\ln(m_{ir})]\\
&\quad+\frac{e}{8\pi}|\vec{u}||\vec{v}|\cos(\beta)[-\gamma_{\rm euler}+\ln(2)-\ln(r)-\ln(m_{ir})]+\frac{e}{4\pi}|\vec{u}||\vec{v}|\cos(\beta-2\alpha), \qquad (23)
\end{aligned}
$$

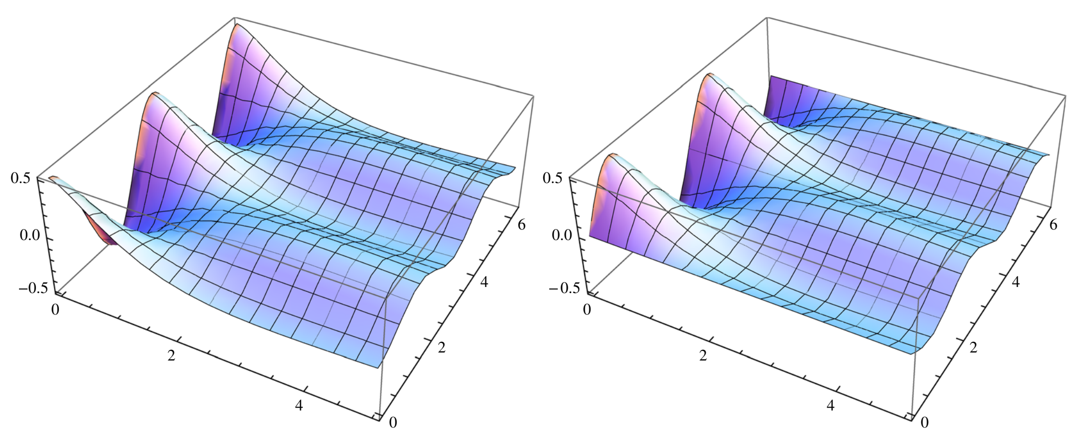

(a) (b)

FIG. 4. Contribution to the electrostatic potential $\frac{A^0_{\rm cl}}{(e/2\pi)|\vec{u}||\vec{v}|}$ (z axis) vs $m_{\rm cs}r$ (x axis) vs α (y axis), in the anisotropic case with $m_{\rm cs}\neq 0$. (a) Collinear $\vec{u}$ and $\vec{v}$; (b) perpendicular $\vec{u}$ and $\vec{v}$.

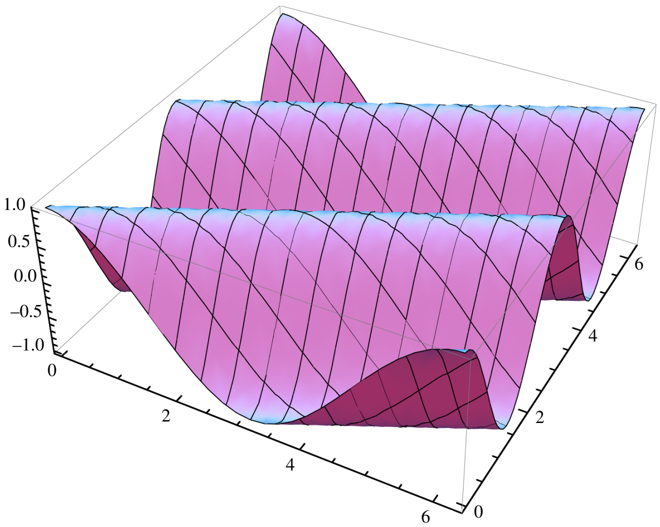

FIG. 5. Contribution to the electrostatic potential $\frac{A^0_{\rm cl}}{(e/4\pi)|\vec{u}||\vec{v}|}$ (z axis) vs β (x axis) vs α (y axis), in the anisotropic case with $m_{\rm cs} = 0$.

where $\gamma_{\rm euler} = 0.577$ is the Euler-Mascheroni constant and m_{ir} is an infrared regulator.[3]

The first and second terms in (23) recover the typical logarithmic potential of planar Maxwell electrodynamics, corrected by the space-time anisotropy introduced by the trivectors u^μ and v^μ. In the third term, as occurs in (20), the spatial anisotropy adds an angular dependence to the potential (23), breaking its circular symmetry, as depicted in Fig. 5.

B. Planar Uehling potential with isotropic Lorentz violation

The quantum fluctuations of the electromagnetic vacuum modify the photon propagator and contribute to the electrostatic interaction of charged particles. In one-loop approximation, the propagator dressed by quantum corrections is

$$iD'_{F\mu\nu}(k) = iD_{F\mu\nu}(k) + iD_{F\mu\alpha}(k) i\Pi^{\alpha\beta}(k) iD_{F\beta\nu}(k), \quad (24)$$

where the first term is the classical propagator (16) and the second encompasses the vacuum polarization contribution.

The vacuum polarization tensor, at one-loop, writes

$$i\Pi_{\mu\nu}(k) = -e^2 \int \frac{d^3p}{(2\pi)^3} \mathrm{Tr}[\gamma_\mu S_0(p)\gamma_\nu S_0(p-k)], \quad (25)$$

with the fermion propagator of our chiral model [8]

$$S_0(p) = \frac{\not{p} + m_o\tau}{p^2 - m_o^2 + i\epsilon}. \quad (26)$$

Decomposing (25) in its symmetric and antisymmetric parts, gives

$$\begin{aligned} i\Pi^{\rm SYM}_{\mu\nu}(k) = &-4e^2[2J^{(3)}_{\mu\nu}(k) - k_\nu J^{(2)}_\mu(k) \\ &- k_\mu J^{(2)}_\nu(k) + g_{\mu\nu}k^\alpha J^{(2)}_\alpha(k) \\ &+ m_o^2 g_{\mu\nu}J^{(1)}(k) - g_{\mu\nu}g^{\alpha\beta}J^{(3)}_{\alpha\beta}(k)], \end{aligned} \quad (27)$$

$$i\Pi^{\rm ASYM}_{\mu\nu}(k) = -4ie^2 m_o k^\alpha \epsilon_{\alpha\mu\nu} J^{(1)}(k), \quad (28)$$

written in terms of the auxiliary integrals

$$J^{(1)}(k) = \int \frac{d^3p}{(2\pi)^3} \frac{1}{p^2 - m_o^2} \frac{1}{(p-k)^2 - m_o^2}, \quad (29)$$

$$J^{(2)}_\alpha(k) = \int \frac{d^3p}{(2\pi)^3} \frac{1}{p^2 - m_o^2} \frac{p_\alpha}{(p-k)^2 - m_o^2}, \quad (30)$$

$$J^{(3)}_{\alpha\beta}(k) = \int \frac{d^3p}{(2\pi)^3} \frac{1}{p^2 - m_o^2} \frac{p_\alpha p_\beta}{(p-k)^2 - m_o^2}. \quad (31)$$

In the low-energy (long-range) limit, defined by $k^2 \ll m_o^2$, the integrals (29)–(31) result in [8]

$$J^{(1)}(k) = \frac{i}{8\pi\sqrt{k^2}} \ln\left(\frac{2m_o + \sqrt{k^2}}{2m_o - \sqrt{k^2}}\right), \quad (32)$$

$$J^{(2)}_\alpha(k) = \frac{i}{16\pi\sqrt{k^2}} \ln\left(\frac{2m_o + \sqrt{k^2}}{2m_o - \sqrt{k^2}}\right) k_\alpha, \quad (33)$$

$$\begin{aligned} J^{(3)}_{\alpha\beta}(k) = &\frac{i}{16\pi}\left[m_o + \frac{1}{4\sqrt{k^2}}(4m_o^2 - k^2)\ln\left(\frac{2|m_o| + \sqrt{k^2}}{2|m_o| - \sqrt{k^2}}\right)\right] g_{\alpha\beta} \\ &+ \frac{i}{16\pi k^2}\left[m_o - \frac{1}{4\sqrt{k^2}}(4m_o^2 - 3k^2)\ln\left(\frac{2m_o + \sqrt{k^2}}{2m_o - \sqrt{k^2}}\right)\right] \\ &\times k_\alpha k_\beta, \end{aligned} \quad (34)$$

which define completely the polarization tensor (27), (28).

From the low-energy polarization tensor we can extract the quantum correction to the long-range electrostatic potential through the dressed propagator [13],

$$A^0_{\rm q}(\vec{k}) = -eD_{0\mu}(0,\vec{k}) i\Pi^{\mu\nu}(\vec{k}) iD_{\nu 0}(0,\vec{k}), \quad (35)$$

providing a Lorentz-violating planar version of the Uehling potential of QED$_4$ [13,14]. Here we highlight the isotropic violation scenario, $u^\mu = (u^0, \vec{0})$ and $v^\mu = (v^0, \vec{0})$, reserving the issue of spatial anisotropy for a future communication.

[3]Naturally, the constant terms in the potentials (23) and (39) have no physical meaning and can be absorbed in the infrared regulator by the redefinition $m_{ir} = \tilde{m}_{ir} 2e^{-\gamma_{\rm euler}}$.

1. Case $m_{\mathrm{cs}} \neq 0$

From (16), in the isotropic case, and the one-loop polarization tensor, the long-range potential (35) in the momentum space up to second order in $|\vec{k}|/m_o$ can be expressed as

$$A_{\mathrm{q}}^{0}(\vec{k}) = -\frac{e^3}{6\pi}\frac{m_{\mathrm{cs}}}{m_o}(m_{\mathrm{cs}}+6m_o)\frac{1}{(m_{\mathrm{cs}}^2+\vec{k}^2)^2} + \frac{e^3}{12\pi}\frac{m_{\mathrm{cs}}+2m_o}{m_o^2}\frac{\vec{k}^2}{(m_{\mathrm{cs}}^2+\vec{k}^2)^2} + \frac{5e^3}{4\pi}\frac{m_{\mathrm{cs}}^3}{(m_{\mathrm{cs}}^2+\vec{k}^2)^3}u_0 v_0 - \frac{e^3}{48\pi}\frac{1}{m_o^2}(5m_{\mathrm{cs}}^3+28m_{\mathrm{cs}}^2 m_o - 12 m_{\mathrm{cs}} m_o^2)\frac{\vec{k}^2}{(m_{\mathrm{cs}}^2+\vec{k}^2)^3}u_0 v_0 - \frac{e^3}{48\pi}\frac{m_{\mathrm{cs}}+12m_o}{m_o^2}\frac{(\vec{k}^2)^2}{(m_{\mathrm{cs}}^2+\vec{k}^2)^3}u_0 v_0 + O(|\vec{k}|^3/m_o^3). \tag{36}$$

Performing the Fourier transform to the position space, we arrive at the corrected potential

$$\begin{aligned} A_{\mathrm{q}}^{0}(\vec{r}) = & -\frac{e^3}{12\pi^2}\frac{m_{\mathrm{cs}}+6m_o}{m_o m_{\mathrm{cs}}}\int_0^\infty \frac{\rho}{(1+\rho^2)^2}\mathrm{J}_0(m_{\mathrm{cs}}\rho r)d\rho + \frac{e^3}{24\pi^2}\frac{m_{\mathrm{cs}}+2m_o}{m_o^2}\int_0^\infty \frac{\rho^3}{(1+\rho^2)^2}\mathrm{J}_0(m_{\mathrm{cs}}\rho r)d\rho \\ & + \frac{5e^3}{8\pi^2}\frac{1}{m_{\mathrm{cs}}}\int_0^\infty \frac{\rho}{(1+\rho^2)^3}\mathrm{J}_0(m_{\mathrm{cs}}\rho r)d\rho u_0 v_0 \\ & - \frac{e^3}{96\pi^2}\frac{1}{m_o^2 m_{\mathrm{cs}}^2}(5m_{\mathrm{cs}}^3+28m_{\mathrm{cs}}^2 m_o - 12 m_{\mathrm{cs}} m_o^2)\int_0^\infty \frac{\rho^3}{(1+\rho^2)^3}\mathrm{J}_0(m_{\mathrm{cs}}\rho r)d\rho u_0 v_0 \\ & - \frac{e^3}{96\pi^2}\frac{m_{\mathrm{cs}}+12m_o}{m_o^2}\int_0^\infty \frac{\rho^5}{(1+\rho^2)^3}\mathrm{J}_0(m_{\mathrm{cs}}\rho r)d\rho u_0 v_0 \\ = & -\frac{e^3}{48\pi^2}\frac{1}{m_o^2}[-2(m_{\mathrm{cs}}+2m_o)\mathrm{K}_0(m_{\mathrm{cs}}r) + (m_{\mathrm{cs}}^2+4m_{\mathrm{cs}}m_o+12m_o^2)r\mathrm{K}_1(m_{\mathrm{cs}}r)] \\ & + \left[-\frac{e^3}{96\pi^2}\frac{5m_{\mathrm{cs}}^3+28m_{\mathrm{cs}}^2 m_o - 12m_{\mathrm{cs}}m_o^2}{m_o^2 m_{\mathrm{cs}}^2}\left(\frac{1}{2}m_{\mathrm{cs}}r\mathrm{K}_1(m_{\mathrm{cs}}r) - \frac{1}{8}m_{\mathrm{cs}}^2 r^2 \mathrm{K}_2(m_{\mathrm{cs}}r)\right)\right. \\ & \left. - \frac{e^3}{96\pi^2}\frac{m_{\mathrm{cs}}+12m_o}{m_o^2}\left(\mathrm{K}_0(m_{\mathrm{cs}}r) - m_{\mathrm{cs}}r\mathrm{K}_1(m_{\mathrm{cs}}r) + \frac{1}{8}m_{\mathrm{cs}}^2 r^2\mathrm{K}_2(m_{\mathrm{cs}}r)\right) + \frac{5e^3}{64\pi^2}m_{\mathrm{cs}}r^2\mathrm{K}_2(m_{\mathrm{cs}}r)\right]u_0 v_0. \end{aligned} \tag{37}$$

The first term in brackets in (37), illustrated in Fig. 6, recovers the quantum potential of the chiral model of QED_3 with Chern-Simons and Haldane terms [8].

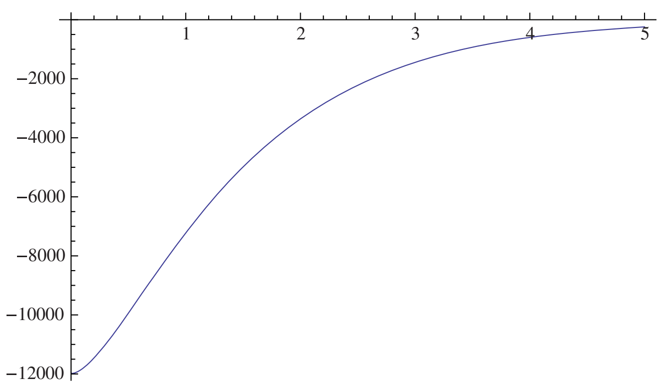

FIG. 6. Quantum correction to the electrostatic potential $\frac{A_{\mathrm{q}}^0}{e^3/(48\pi^2 m_o)}$ vs $m_{\mathrm{cs}}r$, with $m_{\mathrm{cs}}/m_o = 0.001$.

The second term in (37), depicted in Fig. 7, singles out the contribution that stems from the isotropic Lorentz violation, which naturally preserves the circular symmetry of the electrostatic potential.

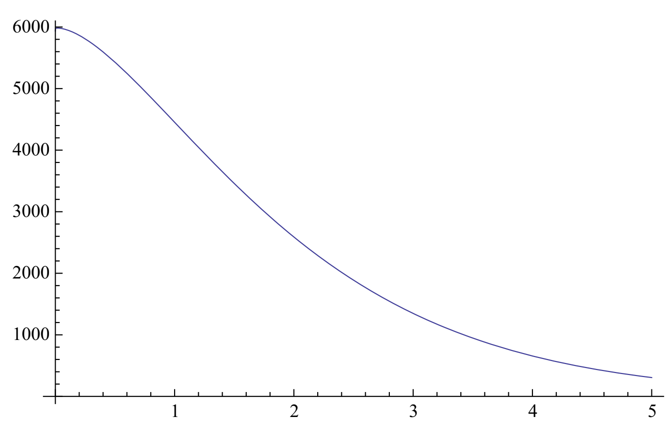

FIG. 7. Quantum correction to the electrostatic potential $\frac{A_{\mathrm{q}}^0}{e^3/(32\pi^2)}$ vs $m_{\mathrm{cs}}r$, with $m_{\mathrm{cs}}/m_o = 0.001$, in the isotropic case.

2. Case $m_{\mathrm{cs}} = 0$

In the absence of the topological photon mass, the momentum-space radiative correction to the long-range electrostatic potential follows from (21) and (35)

$$A^0_{\mathrm{q}}(\vec{k}) = \frac{e^3}{6\pi}\frac{1}{m_o}\left(1 - \frac{11}{2}u_0 v_0\right)\frac{1}{\vec{k}^2} + O(|\vec{k}|^3/m_o^3). \quad (38)$$

Turning to the position space, we find the vacuum polarization contribution

$$\begin{aligned} A^0_{\mathrm{q}}(\vec{r}) &= \frac{e^3}{12\pi^2}\frac{1}{m_o}\left(1 - \frac{3}{2}u_0 v_0\right)\int_0^\infty \frac{\rho}{\rho^2 + m_{ir}^2}\mathrm{J}_0(\rho r)d\rho \\ &= \frac{e^3}{12\pi^2}\frac{1}{m_o}\left(1 - \frac{3}{2}u_0 v_0\right)[-\gamma_{\mathrm{euler}} + \ln(2) \\ &\quad - \ln(r) - \ln(m_{ir})]. \end{aligned} \quad (39)$$

As expected in the isotropic scenario, the circular symmetry of the electrostatic interaction is preserved. Its interesting to note that the long-range radiative correction (39) exhibits the same logarithmic behavior of the classical planar potential of Maxwell electrodynamics.

V. MAGNETIC MOMENT

The electromagnetic vertex introduces the interaction between the photon and the fermion fields trough the gauge principle. This coupling also receives corrections due to fluctuations of the fermion and photon fields as well as from the Lorentz-violating background field dressing the photon propagator, leading, for instance, to a modification in the magnetic moment of the fermion field. Our purpose in this section is to analyze the space-time anisotropy contribution, in one-loop and on-shell approximation and up to second order in the trivectors u^μ and v^μ.

At one-loop order, the electromagnetic vertex correction reads

$$\begin{aligned} &-ie\Gamma_\mu(p', p) \\ &\quad = -ie^3\int\frac{d^3k}{(2\pi)^3}iD^{\nu\alpha}(k)\gamma_\nu iS_0(p'-k)\gamma_\mu iS_0(p-k)\gamma_\alpha. \end{aligned} \quad (40)$$

In the on-shell limit, defined by

$$\not{p}\psi_r(p) = m_o\tau\psi_r(p) \quad (41)$$

$$\bar{\psi}_s(p')\not{p}' = \bar{\psi}_s(p')m_o\tau, \quad (42)$$

and up to second order in the Lorentz violation parameters, in the absence of the Chern-Simons term (i.e., $m_{\mathrm{cs}} = 0$), the vertex (40) can be written as

$$\begin{aligned} -ie\bar{\psi}_s(p')\Gamma_\mu(p', p)\psi_r(p) &= -ie\bar{\psi}_s(p')\Gamma^{(0)}_\mu(p', p)\psi_r(p) \\ &\quad - ie\bar{\psi}_s(p')\Gamma^{(uv)}_\mu(p', p)\psi_r(p), \end{aligned} \quad (43)$$

with

$$-ie\bar{\psi}_s(p')\Gamma^{(0)}_\mu(p', p)\psi_r(p) = -e^3\left(1 + \frac{5}{4}u.v\right)\breve{I}^{(0)}_\mu(p', p), \quad (44)$$

$$\begin{aligned} -ie\bar{\psi}_s(p')\Gamma^{(uv)}_\mu(p', p)\psi_r(p) &= -e^3\breve{I}^{(q)}_{A\mu}(p', p) - e^3\breve{I}^{(q)}_{B\mu}(p', p) \\ &\quad - e^3\breve{I}^{(q)}_{C\mu}(p', p), \end{aligned} \quad (45)$$

where

$$\begin{aligned} \breve{I}^{(0)\mu}(p', p) &= -\int\frac{d^3k}{(2\pi)^3}\frac{1}{k^2}\left(g^{\alpha\nu} - \frac{k^\alpha k^\nu}{k^2}\right)\bar{\psi}_s(p') \\ &\quad \times\gamma_\nu\frac{\not{p}' - \not{k} + m_o\tau}{(p'-k)^2 - m_o^2}\gamma^\mu\frac{\not{p} - \not{k} + m_o\tau}{(p-k)^2 - m_o^2}\gamma_\alpha\psi_r(p), \end{aligned} \quad (46)$$

$$\begin{aligned} \breve{I}^{(q)}_{A\mu}(p', p) &= 2\int\frac{d^3k}{(2\pi)^3}\frac{k.uk.v}{(k^2)^2}\bar{\psi}_s(p')\gamma_\nu\frac{\not{p}' - \not{k} + m_o\tau}{(p'-k)^2 - m_o^2} \\ &\quad \times\gamma_\mu\frac{\not{p} - \not{k} + m_o\tau}{(p-k)^2 - m_o^2}\gamma^\nu\psi_r(p), \end{aligned} \quad (47)$$

$$\begin{aligned} \breve{I}^{(q)}_{B\mu}(p', p) &= \int\frac{d^3k}{(2\pi)^3}\frac{1}{k^2}(u^\alpha v^\nu + u^\nu v^\alpha)\bar{\psi}_s(p') \\ &\quad \times\gamma_\nu\frac{\not{p}' - \not{k} + m_o\tau}{(p'-k)^2 - m_o^2}\gamma_\mu\frac{\not{p} - \not{k} + m_o\tau}{(p-k)^2 - m_o^2}\gamma_\alpha\psi_r(p), \end{aligned} \quad (48)$$

$$\begin{aligned} \breve{I}^{(q)}_{C\mu}(p', p) &= -\int\frac{d^3k}{(2\pi)^3}\frac{1}{(k^2)^2} \\ &\quad \times[k.v(k^\alpha u^\nu + k^\nu u^\alpha) + k.u(k^\alpha v^\nu + k^\nu v^\alpha)] \\ &\quad \times\bar{\psi}_s(p')\gamma_\nu\frac{\not{p}' - \not{k} + m_o\tau}{(p'-k)^2 - m_o^2}\gamma_\mu\frac{\not{p} - \not{k} + m_o\tau}{(p-k)^2 - m_o^2} \\ &\quad \times\gamma_\alpha\psi_r(p). \end{aligned} \quad (49)$$

The vertex contribution to the magnetic dipole interaction comes from [8,13,14] a term proportional to[4] $(1/2)\sigma_{\mu\alpha}\tau q^{\alpha}$, with $\sigma_{\mu\alpha} = (i/2)[\gamma_\mu, \gamma_\alpha]$ and $q_\alpha = p'_\alpha - p_\alpha$. In order to put in evidence the leading contribution, we examine the on-shell vertex (43)–(45) in the forward scattering approximation, defined by $q_\alpha \to 0$.

Therefore, using the Gordon identity [8]

$$\bar{\psi}_s(p')\gamma_\mu\psi_r(p) = \frac{1}{2m_o}\bar{\psi}_s(p')[(p'_\mu + p_\mu)\tau + i\sigma_{\mu\alpha}\tau(p'^{\alpha} - p^{\alpha})]\psi_r(p), \tag{50}$$

reminiscent of the Dirac equation associated with our three-dimensional model, as well as the following identities valid on shell:

$$\bar{\psi}_s(p')[p'.vu^\mu + p'.uv^\mu]\psi_r(p') = m_o\bar{\psi}_s(p')[\not{v}u^\mu + \not{u}v^\mu]\tau\psi_r(p'), \tag{51}$$

$$\bar{\psi}_s(p')[p'.u\not{v} + p'.v\not{u}]p'^\mu\psi_r(p') = \bar{\psi}_s(p')[2p'.up'.v\gamma^\mu]\psi_r(p'), \tag{52}$$

comes the relevant contribution from the vertex terms (46)–(49) to the magnetic dipole moment

$$\Gamma^\mu_{\mathrm{MAG}}(q \to 0) = \Gamma_{\mathrm{MAG}}(q \to 0)\frac{i}{2m_o}\sigma^{\mu\alpha}\tau q_\alpha, \tag{53}$$

with the form factor $\Gamma^\mu_{\mathrm{MAG}}(q \to 0)$ defined by [8]

$$\begin{aligned}\Gamma_{\mathrm{MAG}}(q \to 0) = -ie^2\{&[-4m_o^2X(q \to 0) + 4m_o^2X_{p'}(q \to 0) + 2X_g(q \to 0) + 4m_o^2Y_g(q \to 0) + 4m_o^4Y_{p'p'}(q \to 0)]\\ &+ [-5m_o^2X(q \to 0) + 5m_o^2X_{p'}(q \to 0) + \frac{5}{2}X_g(q \to 0) + 2m_o^2X_{p'p'}(q \to 0) + 13m_o^2Y_g(q \to 0)\\ &+ 5m_o^4Y_{p'p'}(q \to 0) - 4Y_{gg}(q \to 0)]u.v\},\end{aligned} \tag{54}$$

in terms of the auxiliary integrals[5]

$$X(q\to 0) = -\frac{i}{16\pi}\int_0^1 dz_1\int_0^{z_1} dz_2\frac{1}{[m_o^2z_1^2 - m_{ir}^2z_1 + m_{ir}^2]^{3/2}}, \tag{55}$$

$$X_{p'}(q\to 0) = -\frac{i}{16\pi}\int_0^1 dz_1\int_0^{z_1} dz_2\frac{z_1}{[m_o^2z_1^2 - m_{ir}^2z_1 + m_{ir}^2]^{3/2}}, \tag{56}$$

$$X_g(q\to 0) = \frac{i}{16\pi}\int_0^1 dz_1\int_0^{z_1} dz_2\frac{1}{[m_o^2z_1^2 - m_{ir}^2z_1 + m_{ir}^2]^{1/2}}, \tag{57}$$

$$X_{p'p'}(q\to 0) = -\frac{i}{16\pi}\int_0^1 dz_1\int_0^{z_1} dz_2 \times\frac{z_1^2}{[m_o^2z_1^2 - m_{ir}^2z_1 + m_{ir}^2]^{3/2}}, \tag{58}$$

$$Y_g(q\to 0) = -\frac{i}{32\pi}\int_0^1 dz_1\int_0^{z_1} dz_2\int_0^{z_2} dz_3 \times\frac{1}{[m_o^2z_2^2 - m_{ir}^2z_2 + m_{ir}^2]^{3/2}}, \tag{59}$$

$$Y_{p'p'}(q\to 0) = \frac{3i}{32\pi}\int_0^1 dz_1\int_0^{z_1} dz_2\int_0^{z_2} dz_3 \times\frac{z_2^2}{[m_o^2z_2^2 - m_{ir}^2z_2 + m_{ir}^2]^{5/2}}, \tag{60}$$

$$Y_{gg}(q\to 0) = \frac{i}{32\pi}\int_0^1 dz_1\int_0^{z_1} dz_2\int_0^{z_2} dz_3 \times\frac{1}{[m_o^2z_2^2 - m_{ir}^2z_2 + m_{ir}^2]^{1/2}}. \tag{61}$$

Employing the software Mathematica to solve the integral expression for the form factor (54), we find

[4]The interaction energy between an external static electromagnetic field and the fermion field current density, dressed by the one-loop vertex correction, is expressed by [13,14]

$$W = \int_{-\infty}^{\infty} d^2x\bar{\psi}_s(p')[e\gamma_\mu + e\Gamma_\mu(p', p)]\psi_r(p)A^\mu_{\mathrm{ext}}.$$

Using the Gordon identity (50) and considering the external field to be magnetic, the dipole interaction can be written as [8]

$$W = -g\mu_{\mathrm{B}}\int_{-\infty}^{\infty} d^2\vec{x}\bar{\psi}_s(p')\frac{1}{2}\sigma_{12}\tau\psi_s(p)B.$$

From the last expression, we can identify the analogous of the magnetic moment, in our $(2+1)$-dimensional model,

$$\langle\mu^{\mathrm{MAG}}\rangle = g\mu_B\int_{-\infty}^{\infty} d^2\vec{x}\bar{\psi}_s(p')\frac{1}{2}\sigma_{12}\tau\psi_s(p),$$

with $\mu_{\mathrm{B}} = e/(2m_o)$ being the analogous Bohr magneton, and g playing the role of the gyromagnetic ratio.

[5]Planar QED is known to be infrared divergent [15–19]. Therefore, expression (54) is expected to manifest this singular behavior.

$$\Gamma_{\mathrm{MAG}}(q\to 0)=\frac{e^2}{8\pi}\frac{1}{m_o}\left(4+4\ln\left(\frac{m_{ir}}{2m_o}\right)+3\frac{m_o}{m_{ir}}\right)+\frac{e^2}{32\pi}\frac{1}{m_o}\left(10+12\ln\left(\frac{m_{ir}}{2m_o}\right)+7\frac{m_o}{m_{ir}}\right)u.v. \tag{62}$$

In the desired approximation, the corrected gyromagnetic ratio reads [13,14]

$$g=2(1+\Gamma_{\mathrm{MAG}}(q\to 0)). \tag{63}$$

Therefore, defining the fine structure constant $\alpha_{\mathrm{e}}=e^2/m_o$, we recognize the usual QED correction α_{e}/π in the first term of (62), due to the vertex diagram with the bare internal photon. The new feature comes from the second term in the form factor (62) regarding the contribution of the space-time anisotropy from the dressed photon propagator, thus giving a correction of $(5\alpha_{\mathrm{e}}/8\pi)u.v$ for the gyromagnetic ratio.

As anticipated, the infrared regulator is present in the form factor (62) as a consequence of the divergence of the model in that limit [15–19], demanding a renormalization procedure involving *bremsstrahlung* insertions in scattering processes.

VI. CONCLUDING REMARKS

In this work we presented a Standard Model extension based effective model for chiral Maxwell-Chern-Simons QED_3 in the reduced representation, with *CPT*-even Lorentz symmetry violation in the photon sector (1). It was shown that the anisotropy introduced by the Lorentz-breaking parameters supports the magnetoelectric effect in the plane (11)–(13), similarly to the feature investigated in [11] in four dimensions, and the exact bare photon propagator was computed in the employed parametrization 15)). From this propagator, the classical electrostatic potential was determined, up to second order in the Lorentz violation parameters, both in the presence and the absence of the topological photon mass, (20) and (23). In the isotropic violation scenario, the long-range correction, due to the vacuum fluctuations, to the potential was obtained in one-loop approximation, taking into account the Chern-Simons term and omitting its contribution as well, (37) and (39).

The correction to the gyromagnetic ratio (63) due to the anisotropy introduced by the trivectors u^μ and v^μ was calculated from the vertex form factor, (53) and (54), on shell, at one-loop and in the forward scattering approximation, up to first order in the scalar product $u.v$ (62), in the absence of the Chern-Simons interaction.

As future perspectives, the complete analysis of the one-loop radiative corrections, i.e., self-energy and vertex corrections of the model, is in progress [8]. Concerning to the magnetic moment of the fermion, it is desirable to investigate the case where the topological Chern-Simons interaction is also included, employing the photon propagator (16) to determine the modified form factor. In addition, the quantum corrections for the electrostatic potential in the spatially anisotropic scenario are also of phenomenological interest in an interface with condensed matter physics, to be reported. A general parametrization for the Lorentz-violating tensor $R_{\alpha\beta\mu\nu}$, taking into account all its degrees of freedom and having (6) as a particular case, may also unveil a broader scenario and will be a subject of investigation in a near future.

ACKNOWLEDGMENTS

The authors are grateful to the anonymous referee for useful comments and criticism, and for bringing attention to Ref. [11]. G. A. M. A. F. thanks CAPES for the financial support.

APPENDIX: EXACT PHOTON PROPAGATOR COEFFICIENTS

The coefficients $C_k(p)$ that compose the photon propagator (15) are listed here. For brevity, we introduced the quantities

$$\begin{aligned}\mathrm{deno}(C_4)=\{&[16m_{\mathrm{cs}}^2p^2-(p^2(4-5u.v)+8p.up.v)^2]\\&\times[256m_{\mathrm{cs}}^4p^2-32m_{\mathrm{cs}}^2(p^2(p^2(-4+u.v)(-4+5u.v)-8(p.(u\times v))^2)\\&+4p^2(12-7u.v)u.pv.p+32(p.u)^2(p.v)^2)+(p^2(4-5u.v)+8p.up.v)^2\\&\times(16(p.u)^2v^2+p^2((-4+u.v)^2-16u^2v^2)-8(-4+u.v)p.up.v+16u^2(p.v)^2)]\}^{-1}\end{aligned} \tag{A1}$$

and

$$\begin{aligned}\mathrm{deno}(C_5) = {} & \left\{\left[m_{\mathrm{cs}}^2 p^2 - \frac{1}{16}(p^2(4-5u.v)+8u.pv.p)^2\right]\right.\\ & \times\left[-m_{\mathrm{cs}}^4(p^2)^2 + \frac{1}{8}m_{\mathrm{cs}}^2 p^2(p^2(p^2(-4+u.v)(-4+5u.v)-8(p.(u\times v))^2)\right.\\ & +4p^2(12-7u.v)u.pv.p+32(u.p)^2(v.p)^2) - \frac{1}{256}p^2(p^2(4-5u.v)+8u.pv.p)^2\\ & \left.\left.\times(16(u.p)^2v^2+p^2((-4+u.v)^2-16u^2v^2)-8(-4+u.v)u.pv.p+16u^2(v.p)^2)\right]\right\}^{-1}. \end{aligned} \tag{A2}$$

Therefore, the non-null coefficients are

$$C_1(p) = 4\frac{p^2(-4+5u.v)-8p.up.v}{-16m_{\mathrm{cs}}^2p^2+[p^2(-4+5u.v)-8p.up.v]^2}, \tag{A3}$$

$$\begin{aligned}C_2(p) = {} & \frac{1}{(p^2)^2}\left\{\frac{1}{\bar{\zeta}-1} - 4[p^2(-4+5u.v)-8p.up.v]\right.\\ & \times(256m_{\mathrm{cs}}^4(p^2)^2+[p^2(4-5u.v)+8p.up.v]^2[(p^2)^2((-4+u.v)^2-16u^2v^2)\\ & -16p^2(-4+u.v)p.up.v+64(p.u)^2(p.v)^2]-32m_{\mathrm{cs}}^2p^2[(p^2)^2(-4+u.v)(-4+5u.v)\\ & +64(p.u)^2(p.v)^2-8p^2((p.(u\times v))^2-8p.up.v+6u.vp.up.v)])\\ & \times([-16m_{\mathrm{cs}}^2p^2+(p^2(-4+5u.v)-8p.up.v)^2]\\ & \times[256m_{\mathrm{cs}}^4p^2-32m_{\mathrm{cs}}^2(p^2(p^2(-4+u.v)(-4+5u.v)-8(p.(u\times v)^2)\\ & +4p^2(12-7u.v)p.up.v+32(p.u)^2(p.v)^2))\\ & +(p^2(4-5u.v)+8p.up.v)^2(16(p.u)^2v^2+p^2((-4+u.v)^2-16u^2v^2)\\ & \left.-8(-4+u.v)p.up.v+16u^2(p.v)^2)])^{-1}\right\}, \end{aligned} \tag{A4}$$

$$C_3(p) = \frac{16m_{\mathrm{cs}}}{16m_{\mathrm{cs}}^2p^2-[p^2(4-5u.v)+8p.up.v]^2}, \tag{A5}$$

$$\begin{aligned}C_4(p) = {} & -16[p^2(-4+5u.v)-8p.up.v]^2[-16m_{\mathrm{cs}}^2p^2+16im_{\mathrm{cs}}p^2p.(u\times v)\\ & +(p^2(-4+5u.v)-8p.up.v)(p^2(-4+u.v)-4p.up.v)]\mathrm{deno}(C_4), \end{aligned} \tag{A6}$$

$$\begin{aligned}C_5(p) = {} & p^2\left[p^2\left(-1+\frac{5}{4}u.v\right)-2p.up.v\right]^2[-m_{\mathrm{cs}}p^2(m_{\mathrm{cs}}+ip.(u\times v))\\ & +\frac{1}{16}(p^2(-4+5u.v)-8p.up.v)(p^2(-4+u.v)-4p.up.v)]\mathrm{deno}(C_5) \end{aligned} \tag{A7}$$

$$C_6(p) = -p^2\left[p^2\left(-1+\frac{5}{4}u.v\right)-2p.up.v\right]^3[-p^2v^2+(p.v)^2]\mathrm{deno}(C_5), \tag{A8}$$

$$C_7(p) = -64[p^2(4-5u.v)+8u.pv.p]^3[(p.u)^2-p^2u^2]\mathrm{deno}(C_4), \tag{A9}$$

$$C_{10}(p) = -256m_{\mathrm{cs}}[p^2(-4+5u.v)-8u.pv.p]^2[p^2v^2-(p.v)^2]\mathrm{deno}(C_4), \tag{A10}$$

$$C_{11}(p) = 256m_{\mathrm{cs}}[p^2(-4+5u.v)-8u.pv.p]^2[p^2v^2-(p.v)^2]\mathrm{deno}(C_4), \tag{A11}$$

$$\begin{aligned}C_{14}(p) = {} & 64m_{\mathrm{cs}}[p^2(-4+5u.v)-8u.pv.p][16m_{\mathrm{cs}}^2p^2-16im_{\mathrm{cs}}p^2p.(u\times v)\\ & -(p^2(-4+5u.v)-8u.pv.p)(p^2(-4+u.v)-4u.pv.p)]\mathrm{deno}(C_4), \end{aligned} \tag{A12}$$

$$C_{15}(p) = -m_{\mathrm{cs}}p^2\left[p^2\left(-1+\frac{5}{4}u.v\right)-2u.pv.p\right][-m_{\mathrm{cs}}p^2(m_{\mathrm{cs}}+ip.(u\times v)) + \frac{1}{16}(p^2(-4+5u.v)-8u.pv.p)(p^2(-4+u.v)-4u.pv.p)]\mathrm{deno}(C_5), \tag{A13}$$

$$C_{16}(p) = C_{14}(p), \tag{A14}$$

$$C_{17}(p) = 64m_{\mathrm{cs}}[p^2(-4+5u.v)-8u.pv.p][-16m_{\mathrm{cs}}^2p^2-16im_{\mathrm{cs}}p^2p.(u\times v) + (p^2(-4+5u.v)-8u.pv.p)(p^2(-4+u.v)-4u.pv.p)]\mathrm{deno}(C_4), \tag{A15}$$

$$C_{20}(p) = 256m_{\mathrm{cs}}[p^2(4-5u.v)+8u.pv.p]^2[(p.u)^2-p^2u^2]\mathrm{deno}(C_4), \tag{A16}$$

$$C_{21}(p) = -C_{20}(p), \tag{A17}$$

$$C_{22}(p) = \frac{16}{p^2}[p^2(-4+5u.v)-8u.pv.p]^2 \times[64(u.p)^2(v.p)^3+(p^2)^2(-4+5u.v)(4u.pv^2+(-4+u.v)v.p) - 16p^2v.p(m_{\mathrm{cs}}^2+im_{\mathrm{cs}}p.(u\times v)+u.p(2u.pv^2-4v.p+3u.vp.v))]\mathrm{deno}(C_4), \tag{A18}$$

$$C_{23}(p) = \frac{16}{p^2}[p^2(-4+5u.v)-8u.pv.p]^2[64(u.p)^2(v.p)^3 + (p^2)^2(-4+5u.v)(4u.pv^2+(-4+u.v)v.p) - 16p^2v.p(m_{\mathrm{cs}}^2-im_{\mathrm{cs}}p.(u\times v)+u.p(2u.pv^2-4v.p+3u.vp.v))]\mathrm{deno}(C_4), \tag{A19}$$

$$C_{24}(p) = \frac{16}{p^2}[p^2(-4+5u.v)-8u.pv.p]^2[-16m_{\mathrm{cs}}^2p^2u.p+16im_{\mathrm{cs}}p^2u.pp.(u\times v) + (p^2(-4+5u.v)-8u.pv.p)(p^2(-4+u.v)u.p-8(u.p)^2v.p+4p^2u^2v.p)]\mathrm{deno}(C_4), \tag{A20}$$

$$C_{25}(p) = \frac{16}{p^2}[p^2(-4+5u.v)-8u.pv.p]^2[-16m_{\mathrm{cs}}^2p^2u.p-16im_{\mathrm{cs}}p^2u.pp.(u\times v) + (p^2(-4+5u.v)-8u.pv.p)(p^2(-4+u.v)u.p-8(u.p)^2v.p+4p^2u^2v.p)]\mathrm{deno}(C_4), \tag{A21}$$

$$C_{26}(p) = \frac{64m_{\mathrm{cs}}}{p^2}[p^2(-4+5u.v)-8u.pv.p][64(u.p)^2(v.p)^3+(p^2)^2(-4+5u.v)(4u.vv^2+(-4+u.v)v.p) - 16p^2v.p(m_{\mathrm{cs}}^2-im_{\mathrm{cs}}p.(u\times v)+u.p(2u.pv^2-4v.p+3u.vp.v))]\mathrm{deno}(C_4), \tag{A22}$$

$$C_{27}(p) = \frac{64m_{\mathrm{cs}}}{p^2}[p^2(-4+5u.v)-8u.pv.p][64(u.p)^2(v.p)^3+(p^2)^2(-4+5u.v)(4u.vv^2+(-4+u.v)v.p) - 16p^2v.p(m_{\mathrm{cs}}^2+im_{\mathrm{cs}}p.(u\times v)+u.p(2u.pv^2-4v.p+3u.vp.v))]\mathrm{deno}(C_4), \tag{A23}$$

$$C_{28}(p) = -\frac{64m_{\mathrm{cs}}}{p^2}[p^2(-4+5u.v)-8u.pv.p][16m_{\mathrm{cs}}^2p^2u.p+16im_{\mathrm{cs}}p^2u.pp.(u\times v) - (p^2(-4+5u.v)-8u.pv.p)(p^2(-4+u.v)u.p-8(u.p)^2v.p+4p^2u^2v.p)]\mathrm{deno}(C_4), \tag{A24}$$

$$C_{29}(p) = \frac{64m_{\mathrm{cs}}}{p^2}[p^2(-4+5u.v)-8u.pv.p][16m_{\mathrm{cs}}^2p^2u.p-16im_{\mathrm{cs}}p^2u.pp.(u\times v) - (p^2(-4+5u.v)-8u.pv.p)(p^2(-4+u.v)u.p-8(u.p)^2v.p+4p^2u^2v.p)]\mathrm{deno}(C_4), \tag{A25}$$

$$C_{33}(p) = 1024im_{\mathrm{cs}}^2[p^2(-4+5u.v)-8u.pv.p][p^2v^2-(p.v)^2]\mathrm{deno}(C_4), \tag{A26}$$

$$C_{34}(p) = 1024im_{\rm cs}^2[p^2(-4+5u.v) - 8u.pv.p][p^2u^2 - (p.u)^2]\mathrm{deno}(C_4), \tag{A27}$$

$$C_{35}(p) = -256im_{\rm cs}^2[16m_{\rm cs}^2p^2 + 16im_{\rm cs}p^2p.(u\times v) \\ - (p^2(-4+5u.v) - 8u.pv.p)(p^2(-4+u.v) - 4u.pv.p)]\mathrm{deno}(C_4), \tag{A28}$$

$$C_{36}(p) = -256im_{\rm cs}^2[16m_{\rm cs}^2p^2 - 16im_{\rm cs}p^2p.(u\times v) \\ - (p^2(-4+5u.v) - 8u.pv.p)(p^2(-4+u.v) - 4u.pv.p)]\mathrm{deno}(C_4). \tag{A29}$$

[1] D. Colladay and V. A. Kostelecky, *CPT* violation and the Standard Model, Phys. Rev. D **55**, 6760 (1997).

[2] D. Colladay and V. A. Kostelecky, Lorentz-violating extension of the Standard Model, Phys. Rev. D **58**, 116002 (1998).

[3] R. Jackiw and V. A. Kostelecky, Radiatively Induced Lorentz and *CPT* Violation in Electrodynamics, Phys. Rev. Lett. **82**, 3572 (1999).

[4] V. A. Kostelecky and R. Potting, *CPT* and strings, Nucl. Phys. **B359**, 545 (1991).

[5] V. A. Kostelecky and R. Potting, Expectation values, Lorentz invariance, and *CPT* in the open bosonic string, Phys. Lett. B **381**, 89 (1996).

[6] A. Raya and E. D. Reyes, Massive Dirac fermions and the zero field quantum hall effect, J. Phys. A **41**, 355401 (2008).

[7] F. D. M. Haldane, Model for a Quantum Hall Effect without Landau Levels: Condensed-Matter Realization of the Parity Anomaly, Phys. Rev. Lett. **61**, 2015 (1988).

[8] G. A. M. A. Fernandes, Efeitos Planares em Eletrodinâmica Quântica com Violação das Simetrias de Lorentze *CPT*, Ph.D. thesis, Universidade Federal de Santa Catarina, 2018.

[9] R. d'Inverno, *Introducing Einstein's Relativity* (Oxford University Press, New York, 1995).

[10] A. Khare, *Fractional Statistics and Quantum Theory*, 2nd ed. (World Scientific, Singapore, 2005).

[11] Q. G. Bailey and V. A. Kostelecky, Lorentz-violating electrostatics and magnetostatics, Phys. Rev. D **70**, 076006 (2004).

[12] V. A. Kostelecky and N. Russell, Data tables for Lorentz and CPT violation, Rev. Mod. Phys. **83**, 11 (2011).

[13] W. Greiner and J. Reinhardt, *Quantum Electrodynamics*, 3rd ed. (Springer-Verlag, New York, 2003).

[14] M. Schwartz, *Quantum Field Theory and the Standard Model* (Cambridge University Press, Cambridge, England, 2014).

[15] J. L. Tomazelli and B. M. Pimentel, The Green's function in the Bloch-Nordsieck model of QED_3, J. Phys. G **20**, 845 (1994).

[16] J. L. Tomazelli, J. L. Boldo, and B. M. Pimentel, Infrared dynamics in $(2+1)$ dimensions, Can. J. Phys. **76**, 69 (1998).

[17] J. L. Tomazelli, J. L. Boldo, and B. M. Pimentel, Remarks on infrared dynamics in QED in three dimensions, Can. J. Phys. **80**, 1037 (2002).

[18] M. de Roo and K. Stam, Non-perturbative analysis of the infrared properties of QED_3, Nucl. Phys. **B246**, 335 (1984).

[19] W. F. Chen and G. Kunstatter, Constraint from Lamb shift and anomalous magnetic moment on radiatively induced Lorentz and *CPT* violation in quantum electrodynamics, Phys. Rev. D **62**, 105029 (2000).